

## Ambient aerosol sampling using the Aerodyne Aerosol Mass Spectrometer

Jose L. Jimenez,<sup>1,2,3</sup> John T. Jayne,<sup>1</sup> Quan Shi,<sup>1</sup> Charles E. Kolb,<sup>1</sup> Douglas R. Worsnop,<sup>1</sup> Ivan Yourshaw,<sup>4</sup> John H. Seinfeld,<sup>4</sup> Richard C. Flagan,<sup>4</sup> Xuefeng Zhang,<sup>2</sup> Kenneth A. Smith,<sup>2</sup> James W. Morris,<sup>5</sup> and Paul Davidovits<sup>5</sup>

Received 25 July 2001; revised 2 September 2002; accepted 13 September 2002; published 15 April 2003.

[1] The Aerodyne Aerosol Mass Spectrometer (AMS) has been designed to measure size-resolved mass distributions and total mass loadings of volatile and semivolatile chemical species in/on submicron particles. This paper describes the application of this instrument to ambient aerosol sampling. The AMS uses an aerodynamic lens to focus the particles into a narrow beam, a roughened cartridge heater to vaporize them under high vacuum, and a quadrupole mass spectrometer to analyze the vaporized molecules. Particle size is measured via particle time-of-flight. The AMS is operated in two modes: (1) a continuous mass spectrum mode without size information; and (2) a size distribution measurement mode for selected  $m/z$  settings of the quadrupole. Single particles can also be detected and sized if they have enough mass of a chemical component. The AMS was deployed at a ground sampling site near downtown Atlanta during August 1999, as part of the Environmental Protection Agency/Southern Oxidant Study Particulate Matter “Supersite” experiment, and at a suburban location in the Boston area during September 1999. The major observed components of the aerosol at both sites were sulfate and organics with a minor fraction of nitrate, consistent with prior studies and colocated instruments. Different aerosol chemical components often had different size distributions and time evolutions. More than half of the sulfate mass was contained in 2% of the ambient particles in one of the sampling periods. Trends in mass concentrations of sulfate and nitrate measured with the AMS in Atlanta compare well with those measured with ion chromatography-based instruments. A marked diurnal cycle was observed for aerosol nitrate in Atlanta. A simple model fit is used to illustrate the integration of data from several chemical components measured by the AMS together with data from other particle instruments into a coherent representation of the ambient aerosol. **INDEX TERMS:** 0305 Atmospheric Composition and Structure: Aerosols and particles (0345, 4801); 0345 Atmospheric Composition and Structure: Pollution—urban and regional (0305); 0394 Atmospheric Composition and Structure: Instruments and techniques; **KEYWORDS:** aerosols, aerosol mass spectrometer, Aerodyne, particle composition, Atlanta Supersite

**Citation:** Jimenez, J. L., et al., Ambient aerosol sampling using the Aerodyne Aerosol Mass Spectrometer, *J. Geophys. Res.*, 108(D7), 8425, doi:10.1029/2001JD001213, 2003.

### 1. Introduction

[2] Atmospheric aerosols are receiving increasing attention because of their effects on human health, visibility, acid

deposition, and global climate [Seinfeld and Pandis, 1998; Wilson and Spengler, 1996]. Progress in understanding and mitigating these problems is limited by the ability of existing instruments to provide real-time, size-resolved, quantitative measurements of ambient aerosol mass and chemical composition [McMurry, 2000]. A number of measurement techniques possessing some of the required aerosol analysis capabilities have emerged recently. Real-time aerosol mass spectrometers aim to provide information on chemical composition of particle ensembles or individual particles. Most of these instruments also provide information on particle size. A recent review of aerosol measurements by McMurry [2000] states that “these mass spectrometers are, arguably, the most significant development in aerosol measurement in the past 20 years.” Suess and Prather [1999] have recently reviewed the development of this type of instrumentation.

<sup>1</sup>Center for Aerosol and Cloud Chemistry, Aerodyne Research, Inc., Billerica, Massachusetts, USA.

<sup>2</sup>Department of Chemical Engineering, Massachusetts Institute of Technology, Cambridge, Massachusetts, USA.

<sup>3</sup>Now at Department of Chemistry, Cooperative Institute for Research in Environmental Sciences, University of Colorado, Boulder, Colorado, USA.

<sup>4</sup>Department of Chemical Engineering, California Institute of Technology, Pasadena, California, USA.

<sup>5</sup>Department of Chemistry, Boston College, Chestnut Hill, Massachusetts, USA.

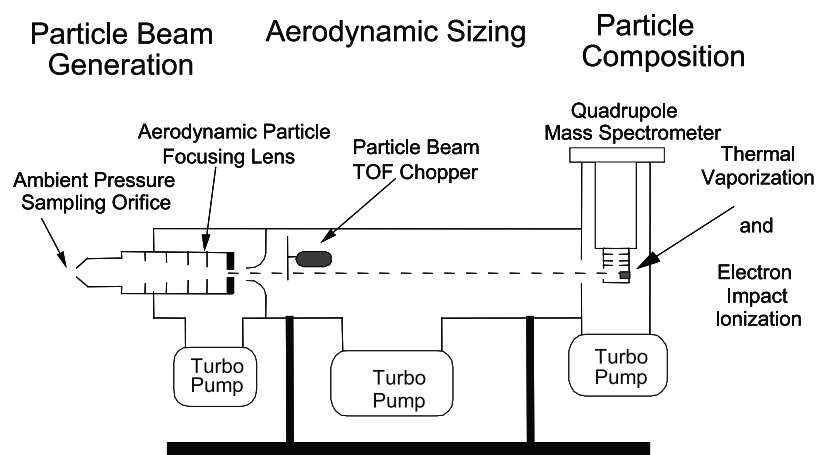


Figure 1. Schematic of the Aerodyne Aerosol Mass Spectrometer (AMS).

[3] We report here on the use of an Aerosol Mass Spectrometer (AMS) developed at Aerodyne Research, which has been designed to provide real-time quantitative information on size-resolved mass loadings for volatile and semivolatile chemical components present in/on ambient aerosol particles [Jayne *et al.*, 2000]. In its present configuration, the AMS cannot detect refractory aerosol components such as sea salt, soil dust, and elemental carbon. Unlike laser-desorption/ionization instruments that provide a qualitative or semiquantitative picture of the full chemical composition of individual particles [Suess and Prather, 1999], the AMS is designed to provide quantitative composition information on ensembles of particles, with limited single particle information. This approach has been shown to provide quantitative detection for laboratory-generated inorganic and organic aerosols [Allen and Gould, 1981; Jayne *et al.*, 2000; Sinha *et al.*, 1982; Tobias *et al.*, 2000]. The present instrument combines standard vacuum and mass spectrometric techniques with recently developed aerosol sampling techniques. A schematic of the AMS is presented in Figure 1. This instrument has been described in detail elsewhere [Jayne *et al.*, 2000] and only a brief summary is provided here.

[4] The AMS consists of three main parts: an aerosol inlet, a particle sizing chamber, and a particle composition detection section. The different sections are separated by small apertures and differentially pumped. The aerosol inlet is based on the design of Liu *et al.* 1995a, 1995b [see also Zhang *et al.*, 2002]. It samples a flow of 1.46 cm<sup>3</sup>/s and focuses particles into a narrow beam (<1 mm diameter). A computational fluid dynamics simulation of the AMS inlet system shows nearly 100% transmission efficiency to the detector for particles in the aerodynamic diameter range 70–500 nm, and shows substantial transmission for particles in the 30–70 nm and 500 nm to 2.5 μm ranges for spherical particles. Irregularly shaped particles may have lower transmission efficiencies [Jayne *et al.*, 2000; Liu *et al.*, 1995a, 1995b; Tobias *et al.*, 2000]. This transmission curve has been verified experimentally for the 100 nm to 1 μm range [Jayne *et al.*, 2000]. Size-dependent particle velocities created by expansion into vacuum are used to determine particle size through a particle time-of-flight measurement. The focused particle beam is modulated by

a rotating wheel chopper operating at about 100 Hz with a ~2% duty cycle. Time-resolved particle detection after a known flight distance gives the particle velocity from which the particle aerodynamic diameter is obtained. Detection is performed by directing the particle beam onto a resistively heated, roughened surface under high vacuum ( $\sim 10^{-7}$  Torr). Upon impact, the volatile and semivolatile components in/on the particles flash vaporize. The vaporization source is integrally coupled to an electron impact ionizer at the entrance of a quadrupole mass spectrometer. When the quadrupole is tuned to a representative mass, bursts of ions are produced that are averaged to produce a size-resolved mass distribution. In addition, when sufficient species mass is present, individual particles can be counted. Such single particle pulses last about 40 μs, a much shorter duration than typical particle time-of-flight ( $\sim 2$ –4 ms). The instrument electronics are coupled to a computer for real-time instrument control and data acquisition, analysis, and display.

[5] The AMS was recently employed to sample ambient aerosols in two different locations in the eastern United States. This paper reports the main results of these measurements, as well as a comparison with collocated instruments. We also present an effective way to integrate the AMS measurements for several  $m/z$ , as well as data from other instruments, into a single coherent description of the ambient aerosol.

## 2. Sampling Locations

[6] The AMS was deployed in Atlanta during August 1999 as part of the first “Supersite” experiment sponsored by the EPA through the Southern Oxidant Study (SOS) [Solomon *et al.*, 2003]. The AMS was located inside one of several trailers, together with a number of other aerosol instruments. Ambient air was sampled through a cyclone designed to transmit particles smaller than 2.5 μm (URG; Chapel Hill, NC) located at a height of 5 m (2 m above the roof of the trailer). Additional ambient sampling was performed in September 1999 in Billerica, Massachusetts, a suburban/rural residential and industrial community about 20 miles NW of downtown Boston. Sampling was performed at the top of a two-story building, with the same PM<sub>2.5</sub> cyclone inlet at the end of a 3 m mast. The suspected

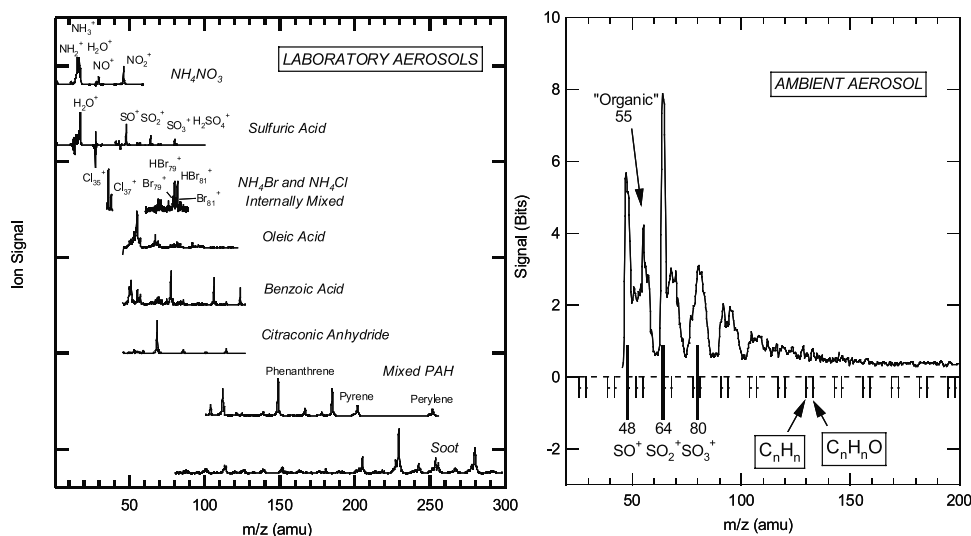


Figure 2. Mass spectra of laboratory and ambient aerosols obtained with the AMS.

major local particle source is Route 3, a highway that is a main Massachusetts-New Hampshire thoroughfare and passes within 100 m of the sampling point.

[7] Previous studies have reported annual average mass concentrations for  $PM_{2.5}$  (particles with an aerodynamic diameter smaller than  $2.5 \mu\text{m}$ ) of  $\sim 7\text{--}10 \mu\text{g}/\text{m}^3$  in rural New England sites and  $16 \mu\text{g}/\text{m}^3$  for an urban site in Boston [Eldred *et al.*, 1997; U.S. Environmental Protection Agency (EPA), 1998]. For rural sites around Atlanta annual averages of  $\sim 12\text{--}13 \mu\text{g}/\text{m}^3$  have been estimated, while an urban site located in nearby Tennessee reported  $\sim 17 \mu\text{g}/\text{m}^3$  [Eldred *et al.*, 1997; EPA, 1998]. For comparison, the new standard proposed by EPA for annual average  $PM_{2.5}$  is  $15 \mu\text{g}/\text{m}^3$ . Ammonium sulfate has been found to be a major component of  $PM_{2.5}$  in the eastern United States, [Baumgardner *et al.*, 1999; Eldred *et al.*, 1997; EPA, 1998]. Aerosol sulfate exhibits a strong seasonal cycle, with the highest concentrations occurring during June, July, and August and the lowest in December, January, and February [Baumgardner *et al.*, 1999]. Carbonaceous material (elemental and organic carbon) is the other major aerosol component, with a larger fraction being found in urban sites than in rural ones [Eldred *et al.*, 1997; EPA, 1998]. Smaller amounts of nitrate and crustal materials are also present [EPA, 1998].

### 3. Modes of Operation and Types of Data Obtained With the AMS

[8] A new data acquisition protocol has been developed for ambient sampling with the AMS. Two modes of operation are alternated. On the “Mass Spectrum” (MS), or “Mass Scanning” mode, the quadrupole is scanned continuously at  $1 \text{ ms}/\text{amu}$  (the maximum rate possible) while sampling ambient aerosol. The particle beam chopper is moved with a computer-controlled stepper motor (every  $\sim 5 \text{ s}$ ) to alternately block the aerosol beam completely or not at all. Difference mass spectra are obtained by subtracting the background signals recorded in the absence of aerosol. The resulting continuous mass spectrum of the chemical species present in the particle ensemble can be

quantified in terms of particle mass for each chemical component. Examples of this type of data for laboratory and ambient aerosols are shown in Figure 2.

[9] In the “Particle Time-of-Flight” (TOF) or “Mass Stepping” mode the quadrupole is set to one of several programmed mass/charge ratios ( $m/z$ ) for a period of time ( $\sim 5 \text{ s}$ ), and then stepped to the next  $m/z$ . The particle beam chopper is operated with  $\sim 2\%$  duty cycle at about  $100 \text{ Hz}$ . Particle aerodynamic diameter is calculated from particle time-of-flight. Typically between 10 and 20  $m/z$  are selected, some of which are based on the expected aerosol composition. In addition, the MS mode provides a systematic, real-time (eventually automatic) basis for optimizing the choice of the  $m/z$  peaks for monitoring in the TOF mode by adding (removing) those peaks that have (do not have) a significant signal in the MS at any given time. Under these conditions, the particle signal is averaged over seconds to minutes (depending on the aerosol loading) to produce a size-resolved mass distribution for each  $m/z$ . An example for  $m/z = 48$  during ambient sampling ( $\text{SO}^+$  from sulfate in this case, see below) is shown in the lower panel of Figure 3. Unlike the counted single particle distribution (see below), the mass distribution obtained by averaging of the analog signal does account for the mass of this species for all the particles that reach the AMS detector. This is a distribution of species mass, that is, the area below the distribution curve is proportional to total mass of the chemical constituent being probed. For unknown mixtures of aerosol chemical components such as in ambient aerosols, it is possible that several chemical components produce ion fragments at the same  $m/z$ . Some checks to detect possible interferences of this type are outlined below.

[10] An additional data processing technique consists of selectively averaging the mass signal for time-of-flight periods when single particles were (were not) detected. For the sulfate data shown in Figure 3 more than half of the sulfate mass (57%) was present in the individually counted particles. The area of the size-resolved mass distribution can be combined with species identification and

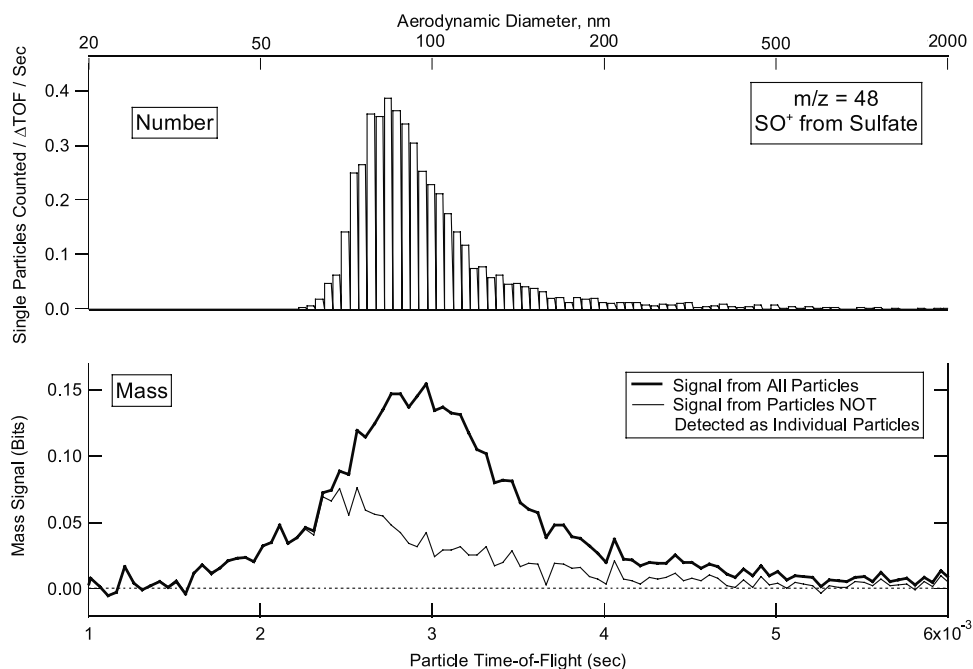


**Figure 3.** Number and mass distributions obtained with the AMS for  $m/z = 48$  ( $\text{SO}^+$  from sulfate, see text) and single particles counted at this  $m/z$ .

instrument calibration data to produce a total mass loading for every averaging time period and chemical component. This procedure is detailed below.

[11] The AMS software also counts and sizes single particles into a size-resolved number distribution for each  $m/z$ . An example is shown in the upper panel of Figure 3. For ambient particles this detected number distribution is biased toward larger particles; e.g., pure component particles need to be about 200 nm or larger to be counted with 100% efficiency. For example, the counted particles in Figure 3 ( $173 \text{ particles/cm}^3$ ) account for 2.0% of the 8500 particles simultaneously counted with a CPC. Typically between 1 and 5% of the ambient particles will be counted by the AMS at the  $m/z$  with the highest count rate. The reasons for this relatively low count rate are: (1) smaller particles produce signals that are “buried” in the background signal level and cannot be clearly distinguished by the data analysis software as individual particle pulses (although the signal caused by these particles is accounted for properly in the average mass signal described above); and (2) many of the particles may be devoid of the chemical component under study.

[12] The two modes of operation (MS and TOF) are alternated every  $\sim 15$  s. Both modes average their data for 1 to 30 min depending on the ambient aerosol concentration. Higher time resolution (up to 100 Hz) is possible if the aerosol mass loadings are very high. This can be useful for some laboratory studies. Note that only those species that evaporate from the particle heater in less than  $\sim 1$  ms (when on time-of-flight mode) or  $\sim 1$  s (when on mass spectrum mode) are detected. The species vaporization times are experimentally observed to decrease with increasing species vapor pressure and heater temperature. Based on laboratory studies of the temperature needed for fast vaporization of both ammonium nitrate and ammonium sulfate particles, the heater is set to about  $600^\circ\text{C}$  during ambient sampling.

Species with very low vapor pressures such as silicates (from crustal material) and elemental carbon are not detected by the AMS, but more volatile species such as ammonium nitrate or organic acids that are internally mixed with the refractory particles can be detected by the AMS.

#### 4. Chemical Species Identification

[13] Ambient aerosols contain many different chemical species, including hundreds of organic compounds. Aerosol mass spectrometers based on laser desorption/ionization and molecular time-of-flight mass spectrometry or on ion-trap mass spectrometry can obtain a full (although generally non-quantitative) mass spectrum of individual particles [Suess and Prather, 1999]. Off-line instruments such as gas-chromatograph/mass spectrometers [Chaurasia et al., 1995] or the Thermal Desorption Particle Beam Mass Spectrometer [Tobias et al., 2000] attempt to separate the different species prior to introduction into a quadrupole mass spectrometer in order to obtain a full mass spectrum for a species (or group of species) at each elution/desorption time. Because of this separation, the presence of signals corresponding to several fragments of the same molecular species is a strong indication of the presence of that parent species in the particles. In contrast, during real-time operation of the AMS, the quadrupole cannot be tuned across an  $m/z$  range during the time that a signal is produced by a single particle. Only one  $m/z$  is sampled for each particle, so the signal at a given  $m/z$  setting of the quadrupole cannot, in principle, be unequivocally attributed to a given chemical species. Although it would be possible to do so, the thermal desorption technique of Tobias et al. [2000] was not implemented in the AMS because it would require sacrificing the size measurement, the fast time resolution, and the high sensitivity of this instrument that are critical for ambient sampling. It is also possible to replace the quadru-

pole with a time-of-flight mass spectrometer in order to obtain full mass spectra of individual particles, however this has not yet been attempted for the AMS.

[14] This section describes three complementary techniques for the identification and verification of the presence of specific chemical species in ambient aerosol from the AMS data. The first technique relies on comparing the fragmentation patterns of known species with those observed in ambient aerosol. Figure 2 shows several ensemble aerosol mass spectra acquired with the AMS in the laboratory and one of ambient aerosol. A given chemical species produces a well-defined set of  $m/z$  peaks with stable relative peak heights when subjected to electron impact ionization under vacuum. Each laboratory aerosol sampled by the AMS results in a series of  $m/z$  peaks characteristic of its chemical component(s) and the fragmentation pattern of each molecule when subjected to electron impact ionization. For example, sulfuric acid aerosol produces major peaks at  $m/z = 48$  (owing to the  $\text{SO}^+$  ion), 64 ( $\text{SO}_2^+$ ), and 80 ( $\text{SO}_3^+$ ). Ammonium nitrate fragments appear at  $m/z = 30$  ( $\text{NO}^+$ ) and 46 ( $\text{NO}_2^+$ ). Organic components generally fragment more extensively. Most straight-chain carboxylic and dicarboxylic acids, which can be a significant component of ambient aerosols [Limbeck and Puxbaum, 1999; Seinfeld and Pandis, 1998], produce a characteristic peak at  $m/z = 55$  [NIST, 1999], probably  $\text{C}_3\text{H}_3\text{O}^+$ . Organic compounds different from acids that are present in ambient aerosols, such as some aldehydes and  $n$ -alkanes, can also produce an ion fragment at this mass [National Institute of Standards and Technology (NIST), 1999] (from  $\text{C}_3\text{H}_3\text{O}^+$  or  $\text{C}_4\text{H}_7^+$ ) although the relative fraction of this fragment for these species is generally lower than for organic acids.

[15] We have observed all of the above peaks in ambient aerosols. For example the ambient aerosol mass spectrum shown in Figure 2 (recorded in Atlanta) reveals peaks at  $m/z = 48$ , 64, and 80, in relative amounts comparable to those observed with pure  $\text{H}_2\text{SO}_4$  or  $(\text{NH}_4)_2\text{SO}_4$  aerosol (the exact ratios depend on the particular ionization conditions and mass spectrometer used [Bley, 1988]). The “ambient” mass spectrum shown in Figure 2 is consistent with that of aerosol containing sulfate since no other major chemical species is likely to produce the same peaks in similar ratios. This conclusion is also corroborated with data from other instruments indicating that Atlanta aerosols were rich in sulfate during this sampling period [Baumann et al., 2003; Lee et al., 2002; Weber et al., 2003]. The broader groups of peaks in the ambient mass spectrum of Figure 2 (not fully resolved owing to a lower-than-optimal resolution setting on the quadrupole) probably originate from the fragmentation of organic compounds. Again this observation is consistent with other samplers that reported large fractions of organic compounds in the aerosols at this site [Baumann et al., 2003].

[16] The second technique for identifying chemical species is the comparison of size distributions of the signals at different  $m/z$ . In the TOF mode, particle size is measured for the selected  $m/z$  settings. This provides a second test for chemical species identification in the form of size distributions at different  $m/z$  settings of the quadrupole: fragments originating from the same species must have the same size distribution. Figure 4 shows such mass size distributions for ambient sampling in Billerica, Massachusetts, on 14 September 1999. The area between zero signal and a given size

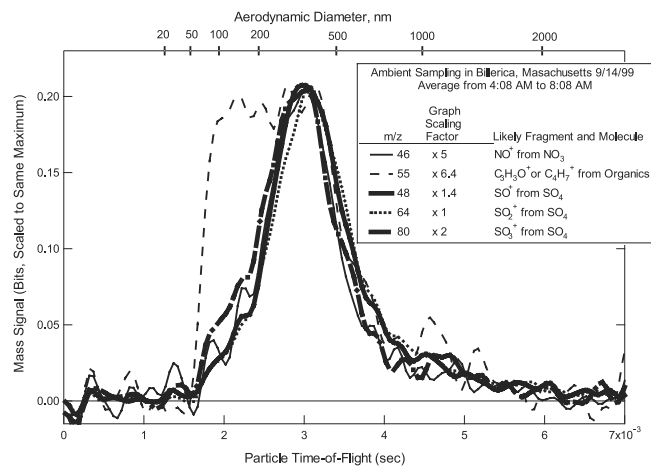


**Figure 4.** Size distributions of particle mass at several quadrupole mass/charge ratios for the average of 4 hours of ambient sampling at Billerica, Massachusetts on 14 September 1999. The distributions have been smoothed numerically for easier appreciation of their differences.

distribution for a given size range is proportional to the mass of that chemical component for particles of that size range. The distributions of Figure 4 have been scaled to the peak of the largest signal ( $m/z = 64$ ). The scaling illustrates that the size distributions of  $m/z 48$  and 64 are very similar. This, together with the fragmentation pattern described above, indicates a high likelihood that those signals originate from the  $\text{SO}^+$  and  $\text{SO}_2^+$  fragments of aerosol sulfate. The particle size distribution for  $m/z 46$  (likely  $\text{NO}^+$  from nitrate) is also very close to those of the main sulfate fragments. The amount of nitrate is much smaller than that of sulfate, also consistent with previous studies. The fact that nitrate and sulfate have very similar size distributions indicates that this test is necessary but not sufficient for detection of interferences in AMS data. In contrast, the size distribution for the organic signal ( $m/z = 55$ ) shows the presence of significant mass for smaller particles. The signal at  $m/z 80$  is also very similar to those of  $m/z 48$  and 64, indicating that this signal is likely due to  $\text{SO}_3^+$  from sulfate. For small particle sizes, the results for  $m/z 80$  exhibit a slightly elevated shoulder with respect to results for  $m/z 48$  and 64, which could be indicative of a small (possibly organic) interference for this fragment. The large particle edge of the size distributions is very similar for all components, which could be indicative of an internally mixed aerosol mode. Another indication of possible internal mixing is the presence of small amounts of nitrate in relatively large particles.

[17] A third technique for assessing interferences in AMS data is the examination of the correlation in time of signals from mass peaks of the same species. For example if an interfering species produces a significant signal at one of the  $m/z$  characteristic of sulfate, this  $m/z$  may show lack of correlation in time with the other  $m/z$  of sulfate since both species may originate from different primary emission sources or gas-phase precursors. For the Atlanta Supersite data the signals at  $m/z 48$ , 64, 80, and 81 show good correlation in time, but with higher relative noise for the fragments present in lower amounts (80 and 81). A segment of these data is shown in Figure 5. This indicates that no

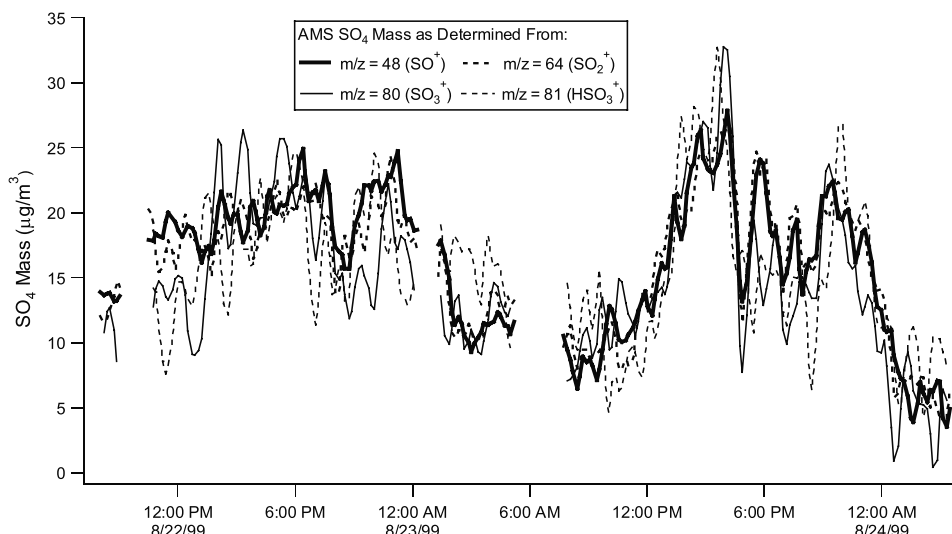


**Figure 5.** Time series of aerosol sulfate mass during the Atlanta experiment as determined from the integration of the AMS mass distributions at  $m/z = 48, 64, 80,$  and  $81$ .

major interferences affected the AMS sulfate measurement in Atlanta during this period. Minor interferences for  $m/z$  80 and 81 cannot be conclusively ruled out with this method owing to the relatively low signal levels (and thus low signal-to-noise ratios) for these peaks.

## 5. Theoretical Basis for the Quantification of Species Mass Concentrations

[18] The signals measured with the AMS can be converted into mass concentrations of aerosol chemical species ( $C_s$ , in  $\mu\text{g}/\text{m}^3$ ) in the following way (adapted from Bley [1988]). The molecular flux  $M_s$  (molecules/s) of species  $s$  entering the AMS detection region per unit time is calculated from the signal at a single  $m/z$  as:

$$M_s = \frac{I_{sf}}{X_{sf} IE_s}, \quad (1)$$

where  $I_{sf}$  is the number of ions detected per unit time at the  $f$ th fragment ( $m/z$ ) of species  $s$ ;  $X_{sf}$  is the fraction of the ions from species  $s$  that are detected at its  $f$ th fragment;  $IE_s$  is the ionization and detection efficiency (total ions detected/molecules vaporized) for species  $s$ .  $IE_s$  is calculated by sampling a known mass flux of monodisperse particles (generated with a Collision atomizer, diffusion dryer, and electrostatic classifier, TSI, St. Paul, Minnesota) and counting them with the AMS and/or with a Condensation Particle Counter (CPC, TSI 3010, St. Paul, Minnesota). If the gain or detection efficiency of the detector (electron multiplier) and/or the transmission efficiency of the quadrupole are a function of the  $m/z$  in the range of interest, these dependences need to be accounted for before using equation (1) by:

$$I_{sf}^{\text{corrected}} = \frac{I_{sf}^{\text{measured}}}{T_{m/z} G_{m/z}}, \quad (2)$$

where  $T_{m/z}$  and  $G_{m/z}$  are the relative quadrupole transmission and the relative response (gain and detection efficiency) of the electron multiplier detector.

[19] The mass concentration of species  $s$  in the aerosol can then be calculated as:

$$C_s = \frac{M_s MW_s}{N_A Q} = \frac{I_{sf}^{\text{corr}}}{N_A Q X_{sf}} \frac{MW_s}{IE_s}, \quad (3)$$

where  $MW_s$  is the molecular weight of species  $s$ ,  $N_A$  is Avogadro's number, and  $Q$  is the air volume sampling rate into the AMS. This procedure assumes that only one species contributes to the signal at that particular  $m/z$ , an assumption that can be tested with the procedures described above. For laboratory experiments with known species,  $MW_s$  is known, while  $IE_s$  and  $X_{sf}$  can be measured with the calibration procedure described above. For unknown species the values for  $IE_s$ ,  $MW_s$ , and  $X_{sf}$  need to be estimated from the available data.  $X_{sf}$  can be estimated from all the detected fragments that have the same time and size evolution and are thus likely to originate from the same species (or group of species). If nothing is known about the molecule,  $IE_s/MW_s$  is assumed to be equal to  $IE_{NO_3}/MW_{NO_3}$ , with  $IE_{NO_3}$  being measured during routine calibration of the AMS. If the chemical nature of the molecule (or group of molecules) is known, e.g., a hydrocarbon, or an oxygenated organic, or an inorganic salt, e.g., by the methods described by McLafferty and Turecek [1993],  $IE_s/MW_s$  is estimated by dividing  $IE_{NO_3}/MW_{NO_3}$  by a response factor (relative to  $NO_3$ ) for that type of molecules ( $R_t$ ).

$$\frac{IE_s}{MW_s} = \frac{1}{R_t} \frac{IE_{NO_3}}{MW_{NO_3}}. \quad (4)$$

And the final expression used to calculate the mass concentration is:

$$C_s = R_t \frac{I_{sf}^{\text{corr}}}{N_A Q X_{sf}} \frac{MW_{NO_3}}{IE_{NO_3}}. \quad (5)$$

[20] Equation (5) is used when the mass concentration of a species is calculated from the signal at a single  $m/z$ . If

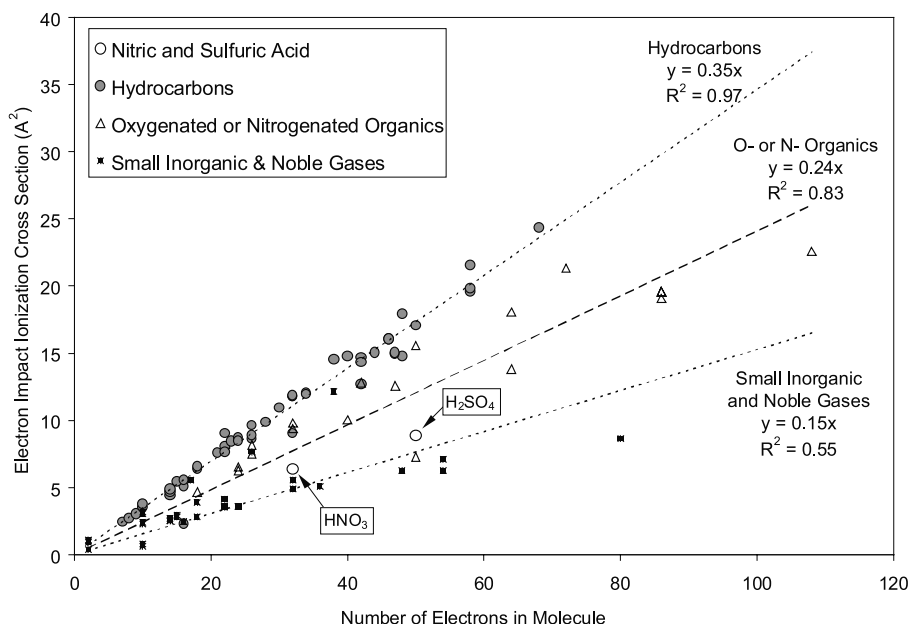


**Figure 6.** Electron impact ionization cross sections of small molecules versus number of electrons in the molecule.

interferences from other species are not important or have been accounted for separately, the signals at all  $m/z$  were a given species produces a signal can be combined in the following alternative expression:

$$C_s = R_t \frac{\sum_f I_{sf}^{corr}}{N_A Q} \frac{MW_{NO_3}}{IE_{NO_3}}. \quad (6)$$

[21] If  $R_t$  is omitted in equations (5) or (6), the resulting mass concentration is known as the “nitrate-equivalent mass” of the species. Care must be taken when using equation (6) so as to not degrade the signal-to-noise for the species mass concentration by including on the average an  $m/z$  with high background noise.

[22] To illustrate the appropriateness and limitations of the assumption regarding relative ionization efficiencies, the data for electron impact ionization cross sections ( $\sigma$ ) with 70 eV electrons is shown in Figure 6 versus the number of electrons in the molecule [Flaim and Ownby, 1971; NIST, 2000; Summers, 1969; K. Irikura, personal communication, 2000]. The ionization efficiency of a molecule is directly proportional to  $\sigma$  since  $\sigma$  merely captures the efficiency of ionization on a per-molecule basis. The number of electrons in a molecule,  $N_e$ , is highly correlated with the molecular weight of the molecule, especially for the volatile and semivolatile molecules present in aerosols. This is owing to the fact that the ratio of atomic number to atomic weight is very similar for most of the atoms involved: 0.50 for C, N, O, S, and Ca; 0.49 for K and Mg; and 0.48 for Na and Cl. The exception is H, which has a ratio of 0.99. The larger value of the atomic ratio for H is neutralized in typical aerosol molecules by the larger contribution of other atoms to the number of electrons and the molecular mass. For example, saturated hydrocarbons have an electron to molecular weight ratio of  $\sim 0.57$ , aromatic hydrocarbons  $\sim 0.54$ , and ammonium nitrate and ammonium sulfate have ratios of 0.52 and 0.53 respectively. Thus, if nothing is known about

the molecule present in the aerosol, it can be assumed that its electron-to-molecular weight ratio is about 0.52 with an uncertainty of about 8%. In summary, since  $IE_s$  is directly proportional to  $\sigma$ , and  $N_e$  is approximately proportional to  $MW_s$ ,  $IE_s/MW_s$  will be proportional to  $\sigma/N_e$ .

[23] Figure 6 shows that  $\sigma/N_e$  is approximately constant for molecules of a given type. From regressions to the data in Figure 6 and approximate  $MW_s/N_e$  ratios for each group of species,  $R_t$  is estimated at 0.51 for hydrocarbons, 0.78 for oxygenated hydrocarbons, and 1.12 for sulfuric acid. Experimental verification of this relative calibration procedure with individual aerosol molecules is undergoing in our laboratory and will be the subject of a future publication.

## 6. Application of the Quantification Procedure to the Massachusetts Data

[24] This procedure has been applied to the 4-hour averages of the size-resolved mass distributions measured for each  $m/z$  setting in Massachusetts (shown in Figures 3 and 4); and the results are shown in Figure 7. The measured number distributions are displayed as well. The largest uncertainty in this case arises from the assumed ionization cross section and fragment fraction of the oxygenated organic component that results in the signal at  $m/z$  55.  $R_t$  is assumed to be equal to 0.78 (oxygenated hydrocarbon) while  $X_{s,55}$  is estimated at  $\sim 18\%$  from fragmentation data for oxygenated organics that have been reported to comprise large mass fractions of the organic aerosol in previous measurements [NIST, 1999; Seinfeld and Pandis, 1998]. The broadening of the distribution produced by the finite opening time of the particle beam chopper and the finite width of the single particle signals can in principle be corrected by using a numerical deconvolution procedure, and also by the modeling approach described below.

[25] The AMS measurements are roughly consistent with prior measurements of  $PM_{2.5}$  in this area. We

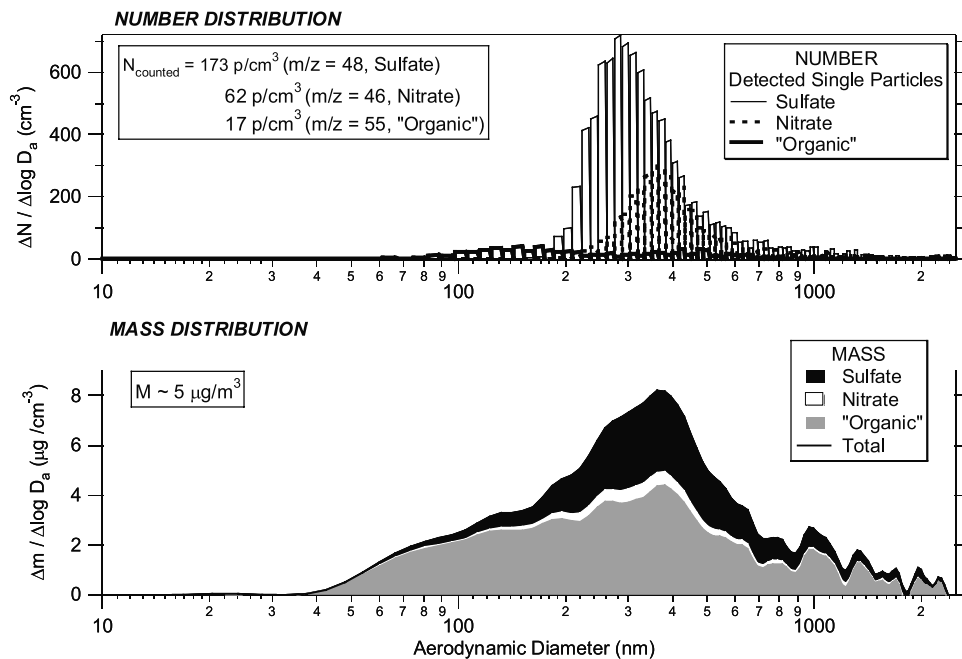


**Figure 7.** Number and mass distributions obtained with the AMS for sulfate, nitrate, and organic aerosol components during ambient sampling in Billerica, MA on 14 September 1999. The mass distributions are stacked on top of each other, while the number distributions are not. The mass distribution accounts for all the particles transmitted into the AMS while the number distributions only account for the particles that produce a large enough signal pulse to be counted individually (<2% of the ambient particles in this experiment).

estimate a mass loading of about  $5 \mu\text{g}/\text{m}^3$  for the sulfate, nitrate, and a portion of the organic component of the aerosol. This is less than the total aerosol mass since crustal constituents and elemental carbon are not included. This result is consistent with reported  $\text{PM}_{2.5}$  annual averages of  $\sim 7\text{--}10 \mu\text{g}/\text{m}^3$  in rural New England sites and  $16 \mu\text{g}/\text{m}^3$  for an urban site in Boston [Eldred *et al.*, 1997; EPA, 1998]. We estimate comparable amounts of sulfate and organics and a much smaller fraction of

nitrate, in agreement with recent ambient measurements [Eldred *et al.*, 1997; EPA, 1998].

## 7. Results From the Atlanta “Supersite” and Comparison to Other Instruments

[26] With the calibration and species identification procedures described above, the AMS can report mass concentrations (in  $\mu\text{g}/\text{m}^3$ ) of volatile and semivolatile aerosol

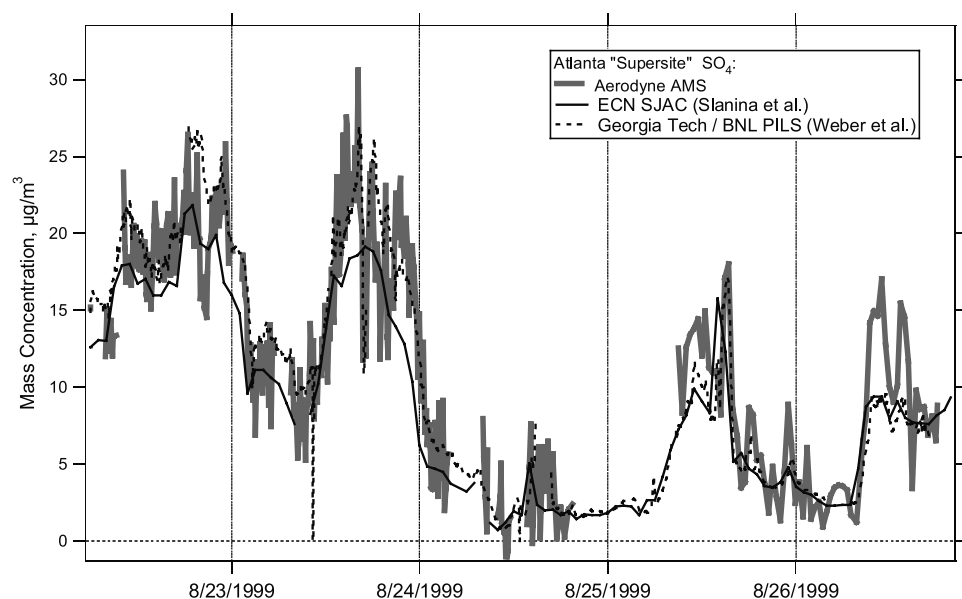


**Figure 8.** Time series of sulfate aerosol mass concentration, as measured by the AMS and by two ion chromatography-based instruments during the Atlanta “Supersite” experiment.



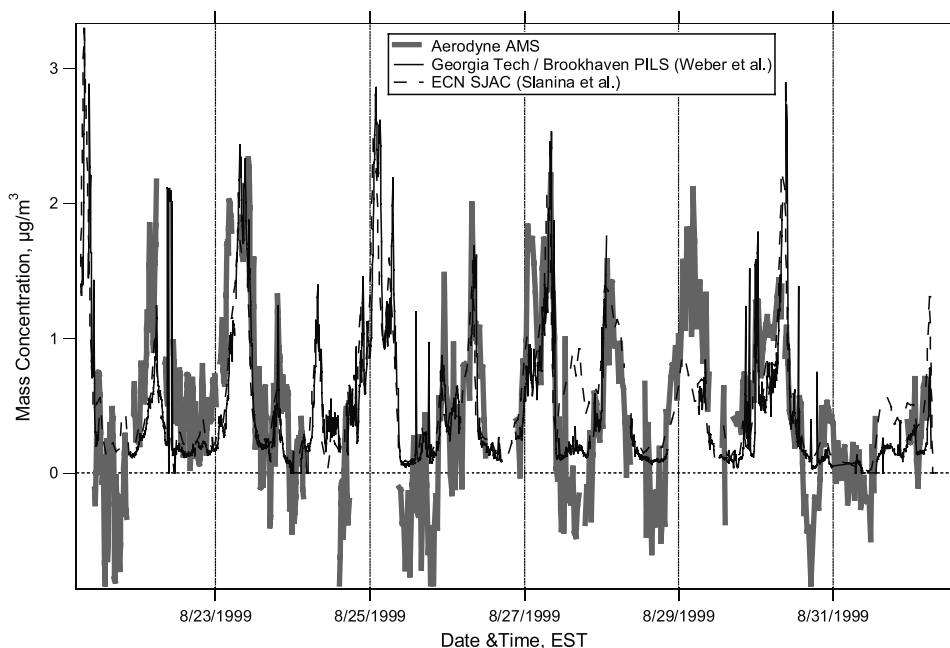


**Figure 9.** Time series of nitrate aerosol mass concentration, as measured by the AMS and by two ion chromatography-based instruments during the Atlanta “Supersite” experiment.

chemical components. The total mass concentrations of  $\text{SO}_4$  and  $\text{NO}_3$  for a portion of the Atlanta campaign are shown in Figures 8 and 9. Unfortunately the size distribution data from this campaign were degraded owing to an irreversible deterioration of the AMS vaporizer that increased the vaporization time to  $\sim 2$  ms. Despite this issue, it was possible to calculate the total mass loadings for the species monitored. During the Atlanta experiment, two ion chromatography-based instruments developed by Weber and coworkers [Weber *et al.*, 2001] and Slanina and coworkers [Khlystov *et al.*, 1995] measured  $\text{PM}_{2.5}$  sulfate and nitrate simultaneously with the AMS measurement. Figures 8 and 9 show the comparison of the measurements of sulfate (from the average of  $m/z$  48 and 64 for the AMS) and nitrate (from  $m/z$  30). After all the calibration factors had been applied, the AMS data for this campaign still needed to be scaled to fit the IC data (using an empirical calibration factor,  $R_{emp}$ , of order 1):

$$C_s^{scaled} = R_{emp} C_s. \quad (7)$$

[27] The need for this additional scaling is suspected to be due to frequent changes in instrument parameters (every few days) in an attempt to compensate for observed sensitivity decreases. Unfortunately the calibration procedures (to determine  $IE_{\text{NO}_3}$ ) were not completely systematized at the time of this campaign and were not performed as often as the instrument tuning was modified. For the 4-day period shown in Figure 8,  $R_{emp}$  was constant at 1.0 (no scaling needed). The AMS results show good correlation with those of the other instruments most of the time, including during some short-lived spikes in the sulfate concentration such as on 8/23/99 around 4 PM and 8/25/99 around 2 PM. The agreement is also reasonable for nitrate as shown in Figure 9, even though the nitrate levels were considerably lower than those of sulfate during this period. A clear diurnal cycle was

observed for nitrate, with maximum levels in the early morning and minimum levels in the afternoon, suggesting that its partitioning into the aerosol phase is favored by lower temperatures and/or higher relative humidities under the conditions of this study. Sulfate lacks a clear diurnal cycle, which is expected since, unlike nitrate, sulfate does not partition into the gas phase.

[28] A direct comparison of the AMS and PILS sulfate measurements in Atlanta is shown in Figure 10. Again this figure indicates the good correlation between both measure-

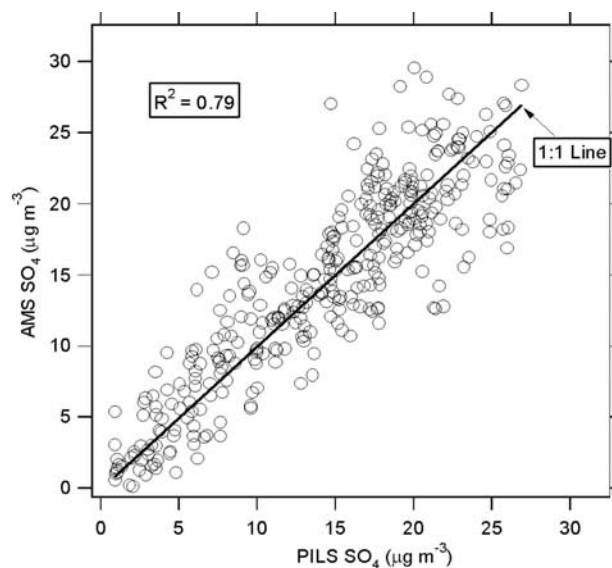


**Figure 10.** Comparison of the AMS and PILS  $\text{SO}_4$  mass concentration measurements during the Atlanta Supersite experiment (from 22 to 28 August 1999).

**Table 1.** Parameters Used for Optimal Fits to the Ambient Data in Figures 9–12

	Mode 1	Mode 2	Mode 3
Particle number, p/cm <sup>3</sup>	8000	475	32
Median diameter, nm	47	165	300
Geometric standard deviation, dimensionless	1.5	1.4	1.5
SO <sub>4</sub> relative mass fraction	10%	40%	48%
NO <sub>3</sub> relative mass fraction	2%	8%	9%
“Organic” relative mass fraction	88%	52%	40%
Mass concentration, µg/m <sup>3</sup>	1.1	2.5	1.3

ments ( $R^2 = 0.79$ ). The correlation coefficient for the nitrate comparison (not shown) is lower owing to the reduced signal to noise of the AMS at the lower concentrations measured ( $R^2 = 0.49$ ).

## 8. Integration of AMS Data for Several Species and Other Concurrent Data

[29] Figure 7 shows a direct conversion of some of the AMS data into size-resolved mass and number distributions. By integrating the mass and number distributions at different  $m/z$  together with data from other available instruments we can develop a more comprehensive description of the ambient aerosol. For this purpose we model the ambient aerosol as a collection of several internally mixed modes, with constant chemical composition within each mode. We then determine the free parameters of the model by minimizing differences between the actual signals and the simulated signals based on the ambient aerosol and AMS models. The ambient number distributions are represented as three lognormal modes as suggested by *Seinfeld and Pandis* [1998]. Each mode is defined by specifying the number of particles per cm<sup>3</sup>, the median diameter and geometric standard deviation of the particle size, and the

mass fraction of each chemical component in all particles of that mode. Non-volatile aerosol components, such as mineral dust or elemental carbon cannot be measured by the AMS and have not been included in the model. If the number distributions are lognormal, it can be shown that the mass distributions are lognormal as well. The AMS model accounts for the measured or calculated particle velocity and transmission/collection efficiency as a function of particle size, and also for the linear mass detection scheme demonstrated for this AMS [*Jayne et al.*, 2000]. It also incorporates a statistical model to represent the probability of single particle detection.

[30] We have used this optimization procedure to integrate the AMS data for all the  $m/z$  measured for the ambient aerosol data taken in Billerica on the morning of 9/14/99. In parallel with the AMS data stream, we also measured total particle concentration using a condensation particle counter (CPC) that read an average of 8500 particles/cm<sup>3</sup> during this period. The total particle number concentration in the model has been constrained by this measurement. The mass and number distributions for the 5  $m/z$  ratios which showed significant signals (48, 64, 80 for sulfate; 46 for nitrate; and 55 for “organic”) have been simulated with this model. The parameters of the model have been adjusted to provide the best fit to the ambient data. The optimum parameters are shown in Table 1. The size distributions that result from the fit for 3  $m/z$  are shown in Figures 11–13. The mass distributions are reasonably well predicted for all  $m/z$ . Modeling of the number distributions of detected particles is inherently more complex than that of the mass distributions owing to the need to represent the statistical variability of single particle signals, and owing to reconciling variations in the actual chemical content of individual particles with the constant composition internal mixture assumed for each mode. The only significant discrepancy appears

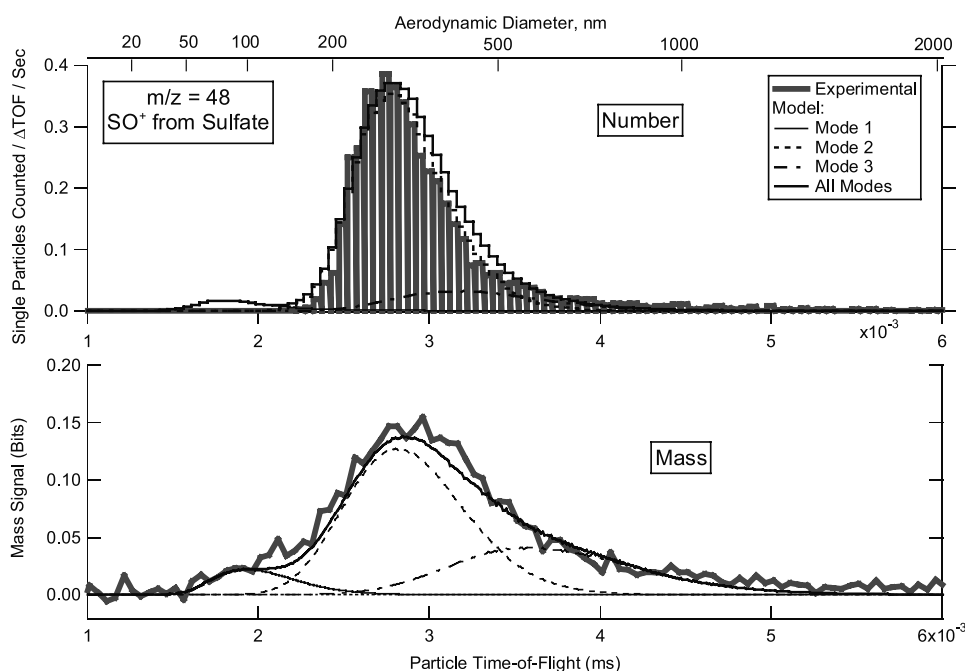


**Figure 11.** Number and mass distributions measured by the AMS for  $m/z = 48$  ( $\text{SO}^+$  from sulfate) and fit to the data with a simple model of the ambient aerosol based on 3 lognormal modes.

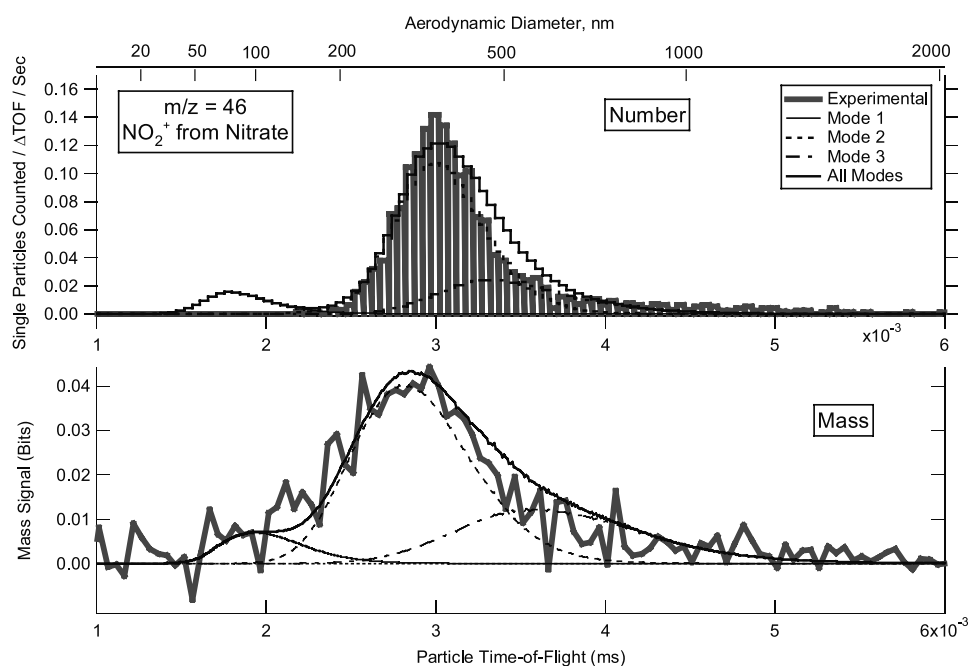


**Figure 12.** Number and mass distributions measured by the AMS for  $m/z = 46$  ( $\text{NO}_2^+$  from nitrate) and fit to the data with a simple model of the ambient aerosol based on 3 lognormal modes.

between the modeled and measured number distributions for the organic signal (Figure 13). This suggests that one the model assumptions (internal mixing of the organic component in the large mode) may be inadequate for particles with that chemical component. The aerosol representation could be refined to include an externally mixed organic aerosol mode. This and other refinements have not been pursued since the data set used here has significant uncertainty for the organic aerosol fraction. The goal of this presentation is

rather to illustrate the type of information that the AMS can provide for ambient aerosols. The number, mass, and chemical composition distributions that provide the best fit to the data are shown in Figure 14. The dashed lines in the figure account for the fraction of the particle number and mass that does not reach the AMS detector, owing to limitations of the particle focusing in the aerodynamic lens inlet at both ends of the size spectrum. According to our model more than 90% of the aerosol particles, but only

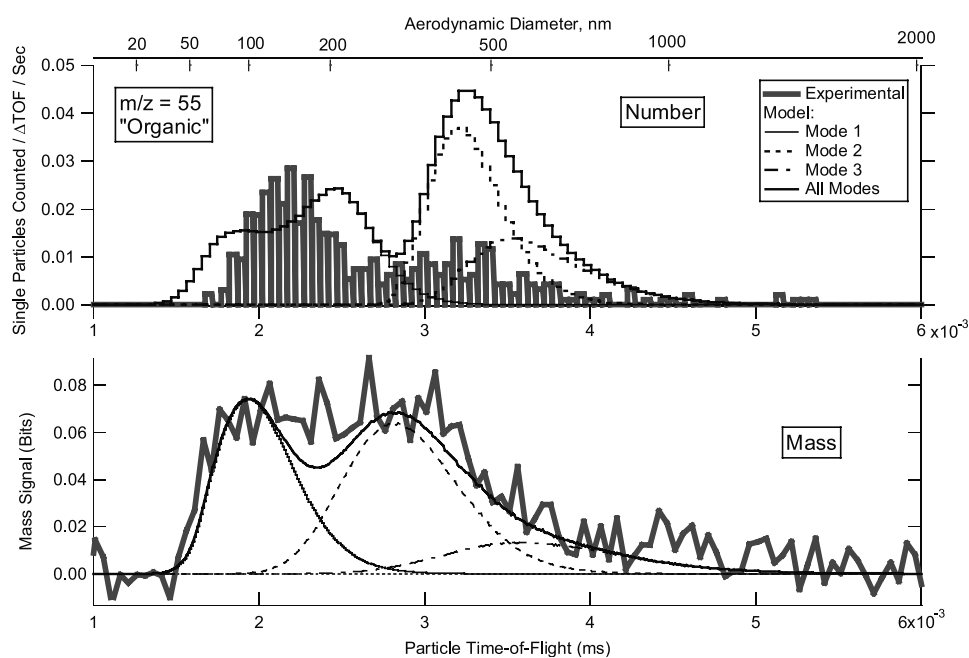


**Figure 13.** Number and mass distributions measured by the AMS for  $m/z = 55$  (organic fragment) and fit to the data with a model of the ambient aerosol based on 3 lognormal modes.

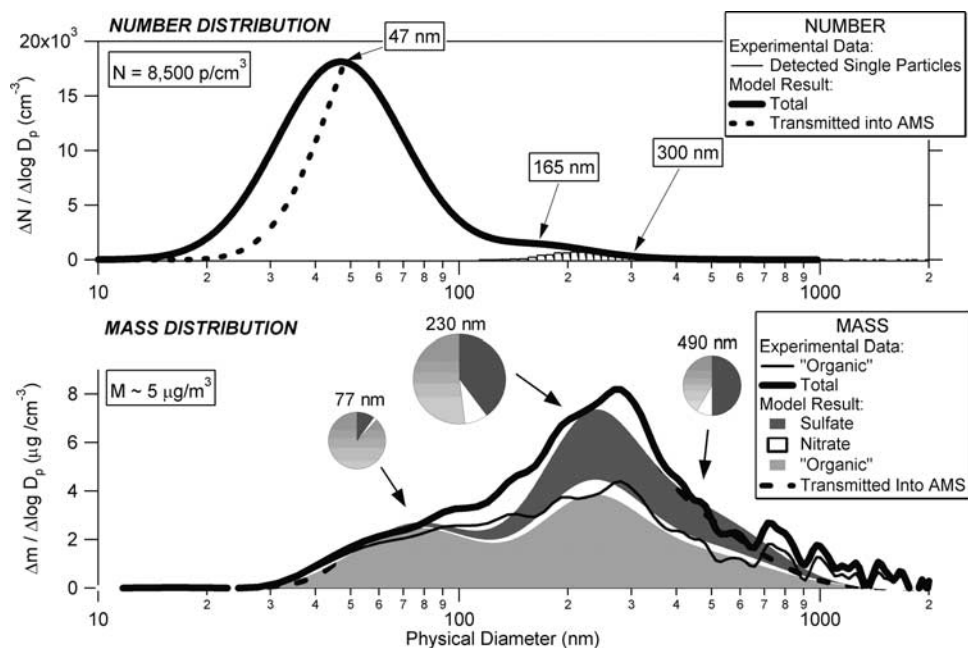


**Figure 14.** Aerosol number, mass, and chemical composition distributions that result in the optimum agreement with a 4-hour average of ambient data (Billerica, MA, 9/14/99). Note that while only  $\sim 2\%$  of the ambient particle number concentration was counted as individual particles by the AMS (typically those  $>200$  nm), the particle mass of the uncounted particles was still measured. The pie charts represent the composition of each of the estimated modes.

$\sim 25\%$  of the measured aerosol mass, was associated with a mostly organic mode centered below 100 nm. A larger “accumulation” mode composed mostly of sulfate, nitrate, and organics comprised a few percent of the particles and about 3/4 of the aerosol mass.

## 9. Conclusions

[31] The Aerodyne Aerosol Mass Spectrometer (AMS) has been used to obtain size and chemical composition information about volatile and semivolatile species in ambient aerosol particles. Sampling was performed at two locations: an urban site in Atlanta, Georgia, during August 1999 and a suburban/rural site in Billerica, Massachusetts, during September 1999. Mass spectrum, mass concentration, and size and chemically resolved mass distribution data were obtained. The major observed components of the aerosol were sulfate and organics with a minor fraction of nitrate at both locations, consistent with prior studies and colocated instruments. No major interferences were present in the measurement of aerosol sulfate. The particle size distributions characterizing different chemical components can be significantly different. Trends in mass concentrations of sulfate and nitrate aerosols in Atlanta agree well with those determined with colocated ion-chromatography-based instruments. Aerosol nitrate showed a marked diurnal cycle in Atlanta, while sulfate did not. More than half of the sulfate mass was contained in 2% of the ambient particles on one of the experiments. A procedure for integrating the AMS number and mass distributions at all  $m/z$  (and data from other instruments) into a coherent description of the ambient aerosol distribution has been demonstrated.

[32] **Acknowledgments.** The authors are grateful to Rodney Weber and Douglas Orsini of the Georgia Institute of Technology (GIT) and Yin-Nan Lee of Brookhaven National Laboratory for the ongoing collaboration that has greatly helped the development and testing of the AMS. We thank Bill Chameides and C.S. Kiang of GIT and Eric Edgerton of Atmospheric Research and Analysis, Inc. for the organization and support of the Atlanta Supersite experiment. We also thank Sjaak Slanina of the Netherlands Energy Research Foundation (ECN) for allowing us to use their data; and Bob Prescott of Aerodyne for his logistical support during the experiments. Financial support for the development of the instrument was provided by the National Science Foundation (grant DMI-9705610) and the Office of Naval Research (grant N00014-98-C-0266). Our participation in the Atlanta field campaign was funded by the EPA/Southern Oxidants Study (grant CR 824849-01).

## References

- Allen, J., and R. K. Gould, Mass spectrometric analyzer for individual aerosol particles, *Rev. Sci. Instrum.*, 52(6), 804–809, 1981.
- Baumann, K., F. Ift, J. Z. Zhao, and W. L. Chameides, Discrete measurements of reactive gases and fine particle mass and composition during the 1999 Atlanta Supersite Experiment, *J. Geophys. Res.*, 108(D7), 8416, doi:10.1029/2001JD001210, 2003.
- Baumgardner, R. E., S. S. Isil, J. J. Bowser, and K. M. Fitzgerald, Measurements of rural sulfur dioxide and particle sulfate: Analysis of CASTNet data, 1987 through 1996, *J. Air Waste Manage. Assoc.*, 49(11), 1266–1279, 1999.
- Bley, W. G., Quantitative measurements with quadrupole mass spectrometers: Important specifications for reliable measurements, *Vacuum*, 38(2), 103–109, 1988.
- Chaurasia, C. S., T. D. Williams, C. M. Judson, and R. P. Hanzlik, Quantitation of fatty-acids and hydroxy fatty-acids by gas chromatography mass spectrometry—Predictively useful correlations of relative response factors with empirical formula, *J. Mass Spectrom.*, 30(7), 1018–1022, 1995.
- Eldred, R. A., T. A. Cahill, and R. G. Floccini, Composition of PM<sub>2.5</sub> and PM<sub>10</sub> aerosols in the IMPROVE network, *J. Air Waste Manage. Assoc.*, 47(2), 194–203, 1997.
- Flaim, T. A., and P. D. Ownby, Observations on Bayard-Alpert ion gauge sensitivities to various gases, *J. Vacuum Sci. Technol.*, 8(5), 861–862, 1971.
- Jayne, J. T., D. C. Leard, X. Zhang, P. Davidovits, K. A. Smith, C. E. Kolb, and D. R. Worsnop, Development of an aerosol mass spectrometer for

- size and composition analysis of submicron particles, *Aerosol Sci. Technol.*, 33(1–2), 49–70, 2000.
- Khlystov, A., G. P. Wyers, and J. Slanina, The steam-jet aerosol collector, *Atmos. Environ.*, 29(17), 2229–2234, 1995.
- Lee, S.-H., D. M. Murphy, D. S. Thomson, and A. M. Middlebrook, Chemical components of single particles measured with Particle Analysis by Laser Mass Spectrometry (PALMS) during the Atlanta Supersite Project: Focus on organic/sulfate, lead, soot, and mineral particles, *J. Geophys. Res.*, 107(D1), 4003, doi:10.1029/2000JD000011, 2002.
- Limbeck, A., and H. Puxbaum, Organic acids in continental background aerosols, *Atmos. Environ.*, 33, 1847–1852, 1999.
- Liu, B. Y. H., P. J. Ziemman, D. B. Kittelson, and P. H. McMurry, Generating particle beams of controlled dimensions and divergence: I. Theory of particle motion in aerodynamic lenses and nozzle expansions, *Aerosol Sci. Technol.*, 22, 293–313, 1995a.
- Liu, B. Y. H., P. J. Ziemman, D. B. Kittelson, and P. H. McMurry, Generating particle beams of controlled dimensions and divergence: II. Experimental evaluation of particle motion in aerodynamic lenses and nozzle expansions, *Aerosol Sci. Technol.*, 22, 314–324, 1995b.
- McLafferty, F. W., and F. Turecek, *Interpretation of Mass Spectra*, Univ. Sci., Mill Valley, Calif., 1993.
- McMurry, P. H., A Review of atmospheric aerosol measurements, *Atmos. Environ.*, 34(12–14), 1959–1999, 2000.
- National Institute of Standards and Technology (NIST), *National Institute of Standards and Technology Chemistry WebBook*, Gaithersburg, Md., 1999. (Available at <http://webbook.nist.gov/chemistry/>.)
- National Institute of Standards and Technology (NIST), *NIST Electron Impact Ionization Cross Section Data Base*, Gaithersburg, Md., 2000. (Available at <http://physics.nist.gov/PhysRefData/Ionization/Xsection.html>.)
- Seinfeld, J. H., and S. N. Pandis, *Atmospheric Chemistry and Physics: From Air Pollution to Climate Change*, John Wiley, New York, 1998.
- Sinha, M. P., C. E. Giffin, D. D. Norris, T. J. Estes, V. L. Vilker, and S. K. Friedlander, Particle analysis by mass spectrometry, *J. Colloid Interface Sci.*, 87(1), 140–153, 1982.
- Solomon, P. A., et al., Overview of the 1999 Atlanta Supersites Project, *J. Geophys. Res.*, 108, doi:10.1029/2001JD001458, in press, 2003.
- Suess, D. T., and K. A. Prather, Mass spectrometry of aerosols, *Chem. Rev.*, 99, 3007–3035, 1999.
- Summers, R. L., Ionization gauge sensitivities as reported in the literature, *NASA Tech. Note TND 5285*, Lewis Res. Cent., NASA, Washington, D. C., 1969.
- Tobias, H. J., P. M. Kooiman, K. S. Docherty, and P. J. Ziemann, Real-time chemical analysis of organic aerosols using a thermal desorption particle beam mass spectrometer, *Aerosol Sci. Technol.*, 33(1–2), 170–190, 2000.
- U.S. Environmental Protection Agency, *National Air Quality and Emissions Trends Report*, Research Triangle Park, N. C., 1998.
- Weber, R., D. Orsini, Y. Duan, Y.-N. Lee, and F. Brechtel, A particle-into-liquid collection for rapid measurement of aerosol bulk chemical composition, *Aerosol Sci. Technol.*, 34, 1900–1905, 2001.
- Weber, R., et al., Short-term temporal variation in PM<sub>2.5</sub> mass and chemical composition during the Atlanta Supersite Experiment, *J. Air Waste Manage. Assoc.*, 53, 84–91, 2003.
- Wilson, R., and J. Spengler, *Particles in Our Air: Concentrations and Health Effects*, Harvard Univ. Press, Cambridge, Mass., 1996.
- Zhang, X., K. A. Smith, D. R. Worsnop, J. L. Jimenez, J. T. Jayne, and C. E. Kolb, A numerical characterization of particle beam collimation by an aerodynamic lens-nozzle system: Part I. An individual lens or nozzle, *Aerosol Sci. Technol.*, 36, 617–631, 2002.

---

P. Davidovits and J. W. Morris, Department of Chemistry, Boston College, Chestnut Hill, MA 02167, USA. (paul.davidovits@bc.edu; colchabert@hotmail.com)

R. C. Flagan, J. H. Seinfeld, and I. Yourshaw, Department of Chemical Engineering, California Institute of Technology, Pasadena, CA 91125, USA. (flagan@caltech.edu; seinfeld@caltech.edu)

J. T. Jayne, C. E. Kolb, Q. Shi, and D. R. Worsnop, Center for Aerosol and Cloud Chemistry, Aerodyne Research, Inc., Billerica, MA 01821-3976, USA. (jayne@aerodyne.com; kolb@aerodyne.com; shiq@aerodyne.com; worsnop@aerodyne.com)

J. L. Jimenez, Department of Chemistry, CIRES, University of Colorado, Boulder, CO 80309, USA. (jose.jimenez@colorado.edu)

K. A. Smith and X. Zhang, Department of Chemical Engineering, Massachusetts Institute of Technology, Cambridge, MA 02139, USA. (kas@mit.edu; zhang@aerodyne.com)